

# FNAL TD Note # TD-06-020

## Linac CH-Type Cavity Section Focusing Solenoid Cold Mass Design

G. Davis, V.V. Kashikhin, T. Page, I. Terechkine, T. Wokas

### I. The solenoid requirements and current design status

After having several iterations of magnetic design followed by beam dynamics simulations, the next set of parameters of a focusing solenoid for the CH-type accelerating section has been negotiated (Table 1):

Table 1: CH-type Section Focusing Solenoid

Number of solenoids in the section	4(MEBT) + 19
<u>Parameter</u>	
Bore diameter (mm)	20
Bore type	warm
Integrated Strength (T <sup>2</sup> ·mm)	1800
Field margin	30%
L <sub>eff</sub> (cm) @ B <sub>m</sub>	< 100 mm
99% Integrated Field Extension	< 2*L <sub>eff</sub>
Available insertion gap (cm)	235 mm

Definitions of the quantities in the table are given below:

- Integrated strength:  $IS = \int_{-\infty}^{+\infty} B_z^2 dz$

- Effective length:  $L_{eff} = \int_{-\infty}^{+\infty} B_z dz / B_0$

The requirement of having limited axial extension of the magnetic field results in a necessity to use bucking coils to bend magnetic flux into an external flux return. The bucking coils, although helping to resolve the fringe field extension problem, require additional space and somewhat reduce field strength in the main coil. This strength reduction can be compensated by increasing the length of the system (if the requirement of the total length can be satisfied) or by using higher magnetic field.

Thorough analysis of the system was needed to meet all the requirements. This analysis started with magnetic modeling. After satisfactory solution was found, preliminary design was suggested and stress analysis was made. Results of this stress analysis required some changes in the system configuration, so several iterations were needed to converge on all major aspects of the solenoid design.

This note describes the status achieved after six iteration cycles. Although it is quite possible that more changes will be made to the design, those changes do not seem significant to us, and we decided to release this note as **a design proposal for the Room Temperature Section Focusing Solenoid**.

### II. Magnetic Design

The primary goal of a magnetic design was to find a sound configuration for a cold mass that meets the solenoid specifications. This design must take into the account parameters of superconducting strand and saturation of a flux return. Because some of the input parameters depend on design features, strand properties, and coil winding

## FNAL TD Note # TD-06-020

patterns, parallel work of making practice coils and using different types of strands for winding was needed. It took several iteration cycles to converge on these parameters.

The current design is based on the next set of winding parameters:

- the main coil is wound in a regular pattern using **an enamel-insulated, round 0.808 mm SSC strand with 0.1 mm insulation** between the layers of winding;
- the bucking coils are wound using round insulated **0.6 mm Oxford strand with 0.1 mm insulation** between the layers of winding.

Compaction factor of the coils is a ratio between the total strand cross-section in the winding and the geometrical coil cross-section. It shows how dense the coil winding is and what engineering current density can be achieved in the windings. Samples of wound coils showed that with some reserve it is safe to use the compaction factor of 0.71 in the main coil and 0.7 mm in the bucking coils. The accepted values of the compaction factor will probably change as we gain experience with winding; additional data obtained during test coil fabrication show a possibility of using the values as high as 0.74. Final choice of a strand will also be made after several practice (test) coils are wound.

Conductor parameters and the solenoid parameters are shown in tables 2 and 3:

Table 2. Conductor parameters.

Parameter	Unit	Main	Bucking
Bare (round) strand diameter	mm	<b>0.808</b>	<b>0.600</b>
Strand insulation thickness	mm	<b>0.025</b>	<b>0.025</b>
Copper to non-copper ratio	-	<b>1.3</b>	<b>1.3</b>
Non-Cu critical current density at 5 T, 4.2 K	A/mm <sup>2</sup>	<b>2750</b>	<b>2750</b>
Engineering current density at 1 A current	A/mm <sup>2</sup>	<b>1.3774</b>	<b>-2.4749</b>

Table 3. Magnet parameters at 4.2K.

Parameter	Unit	Value
Coil aperture	mm	<b>55</b>
Number of turns in the main coil	-	<b>100x26</b>
Number of turns in the bucking coils	-	<b>2x10x37</b>
Average strand packing factor in the main coil	-	<b>0.71</b>
Average strand packing factor in the bucking coils	-	<b>0.70</b>
Yoke length	mm	<b>130</b>
<i>Parameters at FI = 180 T<sup>2</sup>cm</i>		
Magnet current	A	<b>188.04</b>
Central field, $B_0$	T	<b>5.416</b>
Peak field in the coil, $B_{peak}$	T	<b>5.977</b>
Field integral	T <sup>2</sup> cm	<b>180.00</b>
Effective length, $L_{eff}$	mm	<b>81.183</b>
Field integral ratio over $2L_{eff}$	%	<b>99.20</b>
Peak radial field at 10 mm off the axis	T	<b>0.66</b>
Stored energy	kJ	<b>4.445</b>
Magnet inductance	H	<b>0.251</b>
Quench current/nominal current	-	<b>1.33</b>

## FNAL TD Note # TD-06-020

<i>Parameters at quench</i>		
Magnet current	A	<b>250.32</b>
Central field, $B_0$	T	<b>7.156</b>
Peak field in the coil, $B_{peak}$	T	<b>7.894</b>
Field integral, $FI$	$T^2cm$	<b>314.65</b>
Effective length, $L_{eff}$	mm	<b>81.774</b>
Field integral ratio over $2L_{eff}$	%	<b>98.68</b>
Peak radial field at 10 mm off the axis	T	<b>0.87</b>
Stored energy	kJ	<b>7.796</b>
Magnet inductance	H	<b>0.249</b>
Axial force per bucking coil	kN	<b>45.90</b>

A series of figures below show the final magnetic design layout, solenoid load curves with strand critical surfaces, and the longitudinal profile of the magnetic flux density.

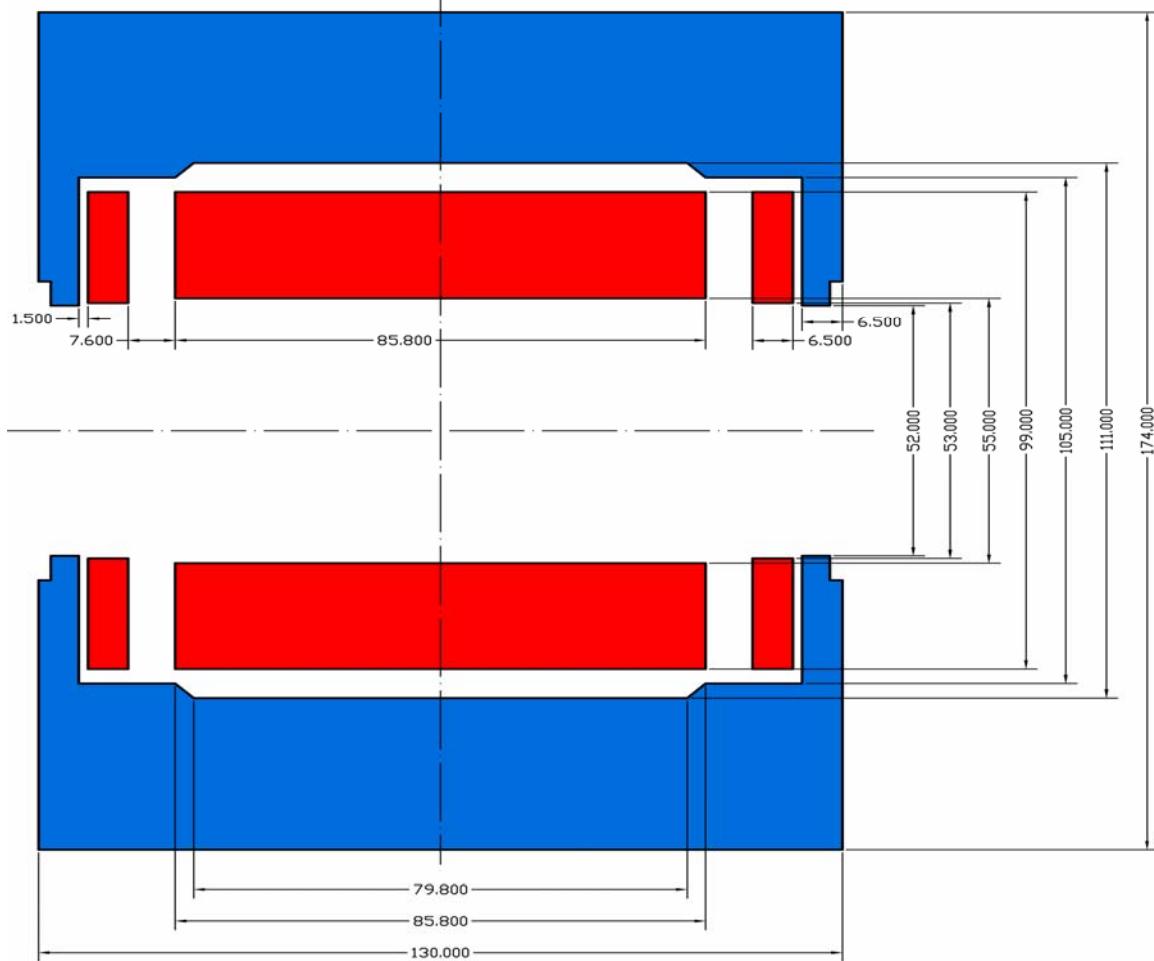


Fig. 1. Cold mass layout

# FNAL TD Note # TD-06-020

Load curves for the main and bucking coils are shown below with the critical surfaces of the used superconducting strand @ 4.2 K:

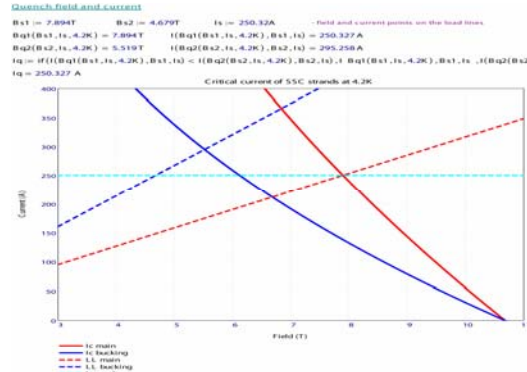


Fig. 2. Critical current diagram

The onset of quench for bucking coils happens at higher strand current, which is a favorable situation because of the high repulsing force applied to the bucking coils and subsequent coil movement and/or deformation.

Longitudinal distribution of the axial magnetic field along the axis is shown in Fig. 3, where the coordinate is in “mm” and the field is in “Tesla”.

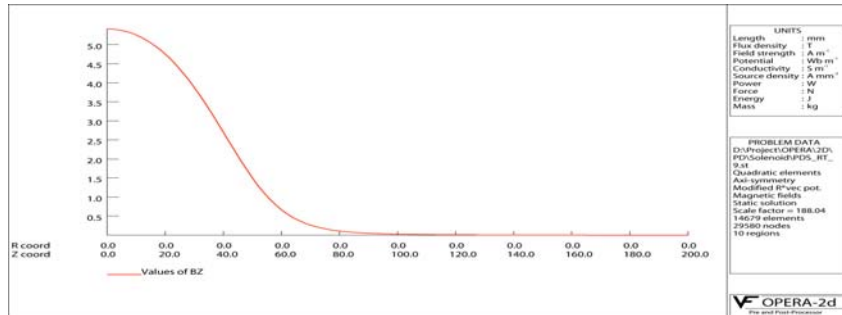


Fig. 3: Axial magnetic field along the axis of the solenoid

It is possible to note quick decay of the residual field outside of the solenoid as a result of compound action of the bucking coils and the flux return.

Radial component of magnetic field (in Tesla) at maximal current along the line parallel to the axis at the distances 10 mm from the axis is shown in Fig. 4. It is important for this component of the field to be kept at a reasonably low level to prevent stripping of H<sup>+</sup> ions accelerated in the linac. In this case, estimate of the effect gives encouraging result of low stripping loss.

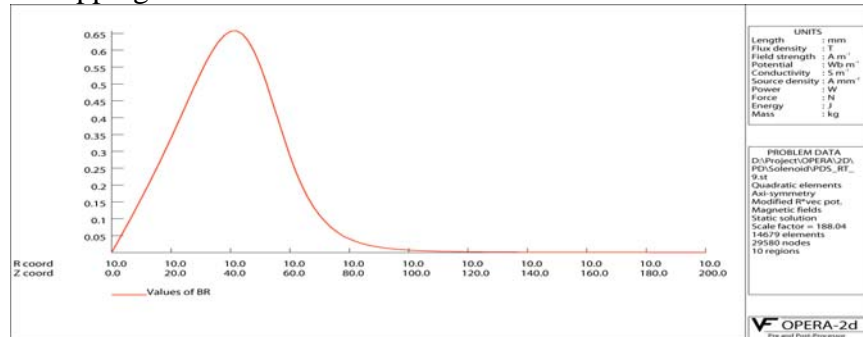


Fig. 4: Radial magnetic field along the axis at the distance of 10 mm from the axis

### III. Mechanical Design

The value of the axial force of ~ 46 kN applied to the bucking coils (see Table 3), although smaller than it was for the first versions of the magnetic design, still is quite high and requires certain measures to prevent movement of the coils. Although allowing using end walls of the flux return to restrict axial movement of the coils (it was not the case during fist iterations), this force required increased thickness of the flux return side walls, which would not be necessary in the case of a small force. The proposed design concept of the solenoid is shown in Fig. 5 below:

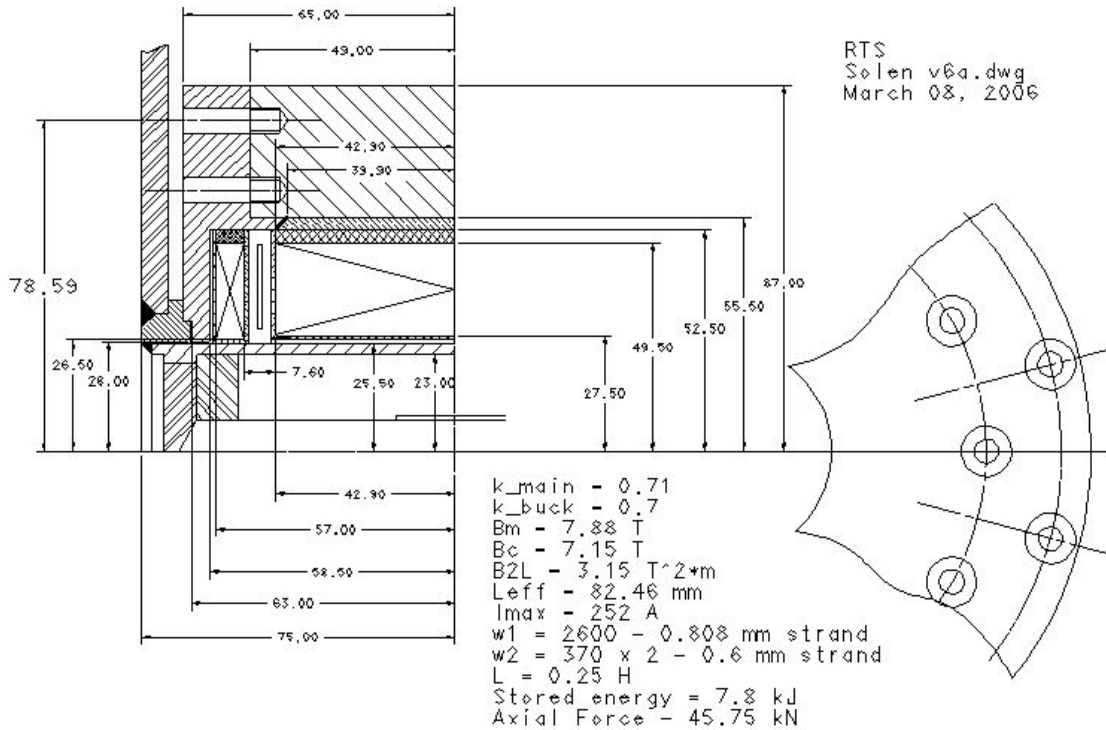


Fig. 5: Solenoid design concept

Main geometry features agree with what is shown in Fig. 1. Thick low-carbon steel flux return side walls are attached to the main flux return by a set of screws capable to withstand the load of about 5,000 lbs (~25 kN). Using only this set of screws would not provide enough rigidity to the system to minimize deformation during the magnet excitation, as can be seen from Fig. 6 (1:100 deformation visualization scale).

The deformation of the inner end of the side wall and the coil reaches ~ 50 mkm; this looks quite high taking into account the relatively small value of the elastic limit for the soft steel. An additional support is needed along the inner radius of the plates.

# FNAL TD Note # TD-06-020

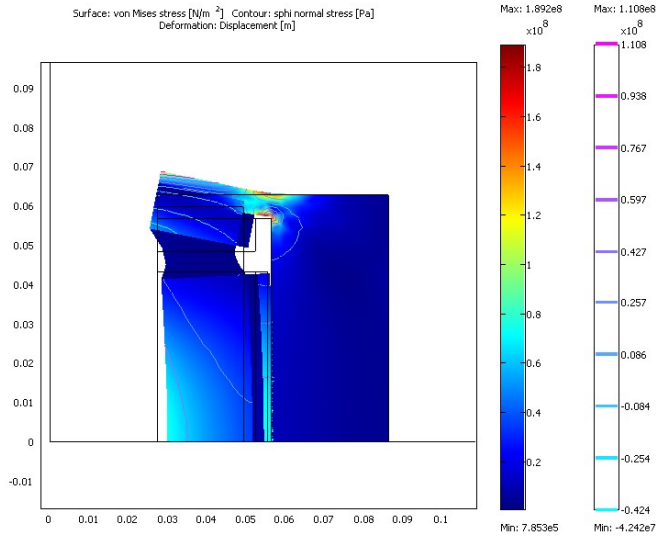


Fig. 6: Deformation of the flux return end plates if not supported from inside.

This support is provided by using an inner pipe of the solenoid's He vessel. When the solenoid is assembled, longitudinal pre-stress of ~ 10 kN is applied to the end plate through a pre-stress ring placed over the He vessel inner pipe. Simultaneously ~ 10 kN of stretching force is applied to the pipe. The pipe and the coil deformation patterns are shown in Fig. 7 (x 100 deformation scale). A graph of the deformation is shown in Fig. 8.

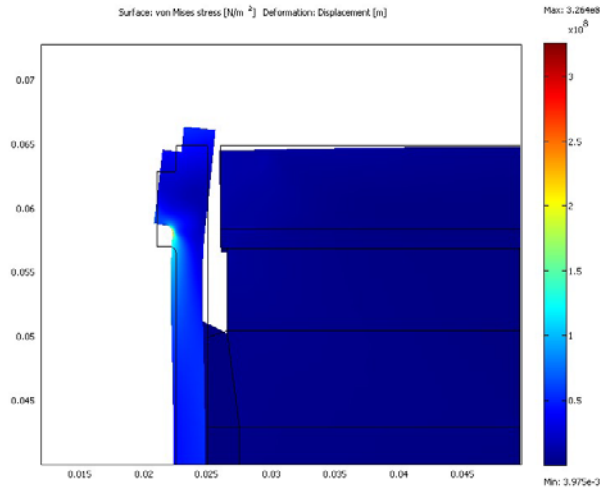
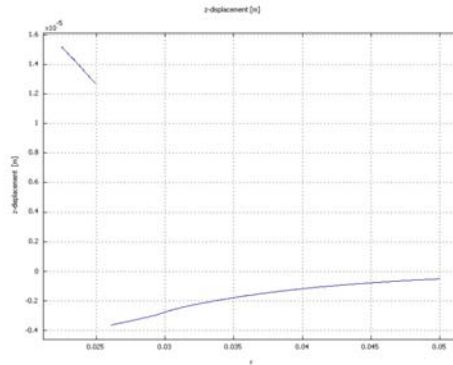


Fig. 7: Stress and deformation during pre-load, before welding



# FNAL TD Note # TD-06-020

Fig. 8: Deformation during pre-load, before welding

This preload should be made using specially designed tooling: a clamp to apply the pre-stress to the solenoid assembly and a jack to stretch the pipe. None of the pieces of the tooling seems challenging because of a quite modest force.

When the pipe is stretched and the pre-stress applied, the ring is to be welded to the pipe before the assembly tooling is removed. Thus, the assembled solenoid has pre-stressed coils and stretched inner pipe. At this point pipe stretching force is applied at different location, and deformation diagram changes compared with Fig. 8

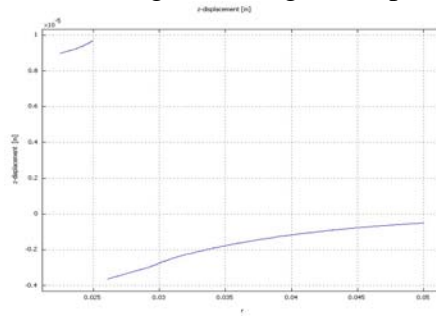


Fig. 9: Deformation diagram after removing the welding fixture.

When excitation current is introduced, the electromagnetic forces will try to push the bucking coils away and further stretch the pipe. Equilibrium at maximal current of 250 A will be reached with the total stretching force of 15 kN. Stress and deformation diagram is shown in Fig. 10, accompanied by the deformation graph in Fig. 11.

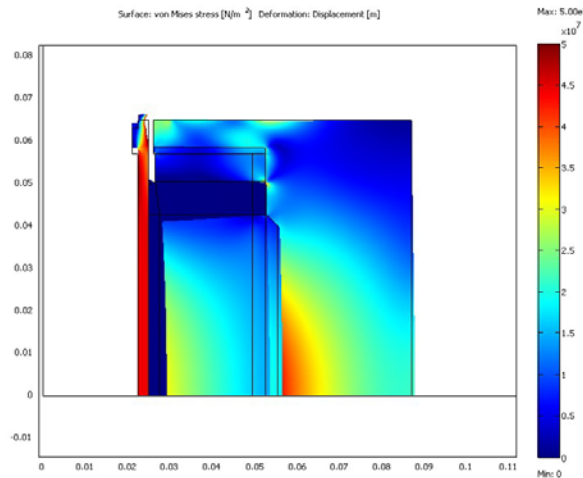
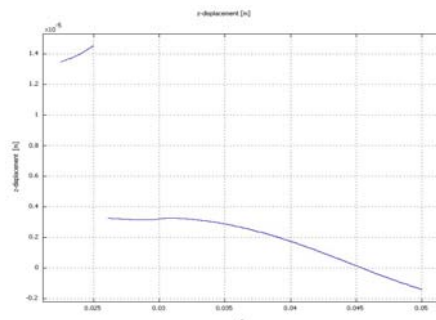


Fig. 10: Stress and deformation diagram at 250 A



## **FNAL TD Note # TD-06-020**

Fig. 11: Deformation at maximal current

Comparing Fig. 11 with Fig. 9, we see that the difference between the axial position of the pipe and the bucking coil is close for both cases. This means that the action of the electromagnetic forces is compensated by stretching the pipe. The absolute value of the deformations is within +/- 5 mkm for the coil and about 15 mkm for the pipe, which seems OK. Maximal stress in the pipe happens near the places where the force is applied and reaches ~200 MPa in spots, which is comparable to the elasticity limit of stainless steel. Choosing stronger steel (e.g. Nitronics) would benefit the design, but even with plain 304 or 316 steel the result looks sufficiently good.

### **IV. Conclusion remarks**

Iterative process of magnetic modeling and mechanical analysis has converged after 6 full iterations resulting in a design that meets both performance and space requirements. The device assembly technique has been suggested that allows minimization of the preload needed for compensates electromagnetic forces.

Design of the device is in the final stage, and will be released for procurement early in May. Nevertheless some issues of the coil design will remain uncertain unless the full cycle of test coils fabrication and testing is completed. Although testing of the first practice coil (PDST-01, the test note pending) provided quite encouraging information about the coil performance, more subtle features like hysteresis performance and spread in compaction factor must be investigated before the design can settle.